

See discussions, stats, and author profiles for this publication at: <https://www.researchgate.net/publication/47565362>

# Impacts of the Canadian Forest Fires on Atmospheric Mercury and Carbonaceous Particles in Northern New York

ARTICLE in ENVIRONMENTAL SCIENCE & TECHNOLOGY · OCTOBER 2010

Impact Factor: 5.33 · DOI: 10.1021/es1024806 · Source: PubMed

CITATIONS

28

READS

62

5 AUTHORS, INCLUDING:



**Yungang (Carl) Wang**

Lawrence Berkeley National Laboratory

36 PUBLICATIONS 386 CITATIONS

SEE PROFILE



**Jiaoyan Huang**

University of North Carolina at Chapel Hill

32 PUBLICATIONS 389 CITATIONS

SEE PROFILE



**Philip K Hopke**

Clarkson University

823 PUBLICATIONS 18,678 CITATIONS

SEE PROFILE



**Thomas M Holsen**

Clarkson University

134 PUBLICATIONS 3,620 CITATIONS

SEE PROFILE

# Characterization of Residential Wood Combustion Particles Using the Two-Wavelength Aethalometer

Yungang Wang,<sup>†</sup> Philip K. Hopke,<sup>\*,†</sup> Oliver V. Rattigan,<sup>‡</sup> Xiaoyan Xia,<sup>†</sup> David C. Chalupa,<sup>§</sup> and Mark J. Utell<sup>§</sup>

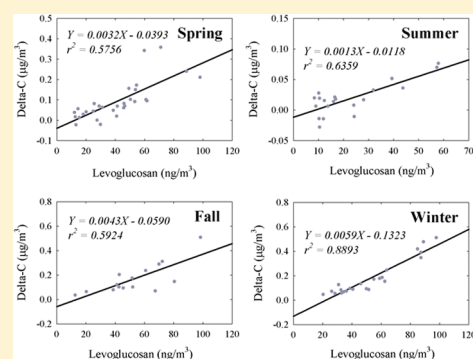
<sup>†</sup>Center for Air Resource Engineering and Science, Clarkson University, Potsdam, New York 13699-5708, United States

<sup>‡</sup>Division of Air Resources, NYS Department of Environmental Conservation, Albany, New York 12233, United States

<sup>§</sup>Departments of Medicine and Environmental Medicine, University of Rochester Medical Center, Rochester, New York 14642, United States

**S** Supporting Information

**ABSTRACT:** In the United States, residential wood combustion (RWC) is responsible for 7.0% of the national primary PM<sub>2.5</sub> emissions. Exposure to RWC smoke represents a potential human health hazard. Organic components of wood smoke particles absorb light at 370 nm more effectively than 880 nm in two-wavelength aethalometer measurements. This enhanced absorption (Delta-C = BC<sub>370 nm</sub> − BC<sub>880 nm</sub>) can serve as an indicator of RWC particles. In this study, aethalometer Delta-C data along with measurements of molecular markers and potassium in PM<sub>2.5</sub> were used to identify the presence of airborne RWC particles in Rochester, NY. The aethalometer data were corrected for the loading effect. Delta-C was found to strongly correlate with wood smoke markers (levoglucosan and potassium) during the heating season. No statistically significant correlation was found between Delta-C and vehicle exhaust markers. The Delta-C values were substantially higher during winter compared to summer. The winter diurnal pattern showed an evening peak around 21:00 that was particularly enhanced on weekends. A relationship between Delta-C and PM<sub>2.5</sub> was found that permits the estimation of the contribution of RWC particles to the PM mass. RWC contributed 17.3% to the PM<sub>2.5</sub> concentration during the winter. Exponential decay was a good estimator for predicting Delta-C concentrations at different winter precipitation rates and different wind speeds. Delta-C was also sensitive to remote forest fire smoke.



## 1. INTRODUCTION

Residential wood combustion (RWC) refers to the burning of wood in fireplaces, woodstoves, and other devices used to heat homes.<sup>1</sup> The major substances in the wood smoke are carbon monoxide (CO), organic gases, PM<sub>2.5</sub> (particulate matter with an aerodynamic diameter less than or equal to 2.5 µm), nitrogen oxides, and sulfur oxides. The particulate fraction is composed of solid or liquid organic compounds, elemental carbon (EC), trace elements (K, S, Cl, etc.), and inorganic ash.<sup>2,3</sup>

Numerous studies reported adverse health effects from breathing RWC smoke. Zelikoff et al. examined the human and animal studies performed over the last three decades.<sup>4</sup> They concluded that exposure to RWC smoke, particularly for children, represents a potential health hazard. With regards to adults, prolonged inhalation of wood smoke contributed to chronic pulmonary disease.

RWC particles are emitted both indoors and outdoors. Approximately 70% of wood smoke from chimneys can actually re-enter the home and neighborhood dwellings.<sup>5</sup> Considering people spend 60–70% of their time at home,<sup>6</sup> RWC smoke poses a substantial human health risk. In the United States, RWC was estimated to account for approximately 7.0% of the national primary PM<sub>2.5</sub> emissions in 2002.<sup>7</sup> These emissions are larger

than the contribution of on-road (2.5%) and are similar to the emissions from off-road (7.3%) mobile sources.

RWC is the largest contributor to PM<sub>2.5</sub> mass in rural areas of New York State particularly during the heating season.<sup>8</sup> Emissions contributions from RWC vary across the continent and are known to be higher in the Northeastern U.S.<sup>9</sup> There were 29 ambient PM<sub>2.5</sub> monitoring stations in New York State in 2008. Since regulatory ambient air monitoring is based on population exposure, these monitors were generally concentrated in urban locations (17 of the 29 stations were located in the NYC metropolitan area) resulting in somewhat sparse coverage across large parts of the state.<sup>10</sup> Thus, the distribution of RWC particles is currently not well-characterized by regulatory monitoring networks.

Organic components of wood smoke particles such as polycyclic aromatic hydrocarbons (PAHs) have been suggested to enhance ultraviolet absorption at 370 nm relative to 880 nm in two-wavelength aethalometer black carbon (BC) measurements.<sup>11</sup>

**Received:** April 23, 2011

**Accepted:** July 20, 2011

**Revised:** July 11, 2011

**Published:** July 20, 2011

This enhanced absorption ( $\Delta C = BC_{370\text{ nm}} - BC_{880\text{ nm}}$ ) can serve as an indicator of RWC and forest fire particles.<sup>12–14</sup> In this paper, two wavelength aethalometer measurements and various copollutant species including levoglucosan and potassium were used to assess RWC particles in Rochester, NY.

## 2. EXPERIMENTAL METHODS

Rochester, located on the shores of Lake Ontario, is the third largest city in New York State. In 2010, it had a population of 210,565 (U.S. Census Bureau, <http://www.census.gov/>). The greater Rochester metropolitan area has a population of more than one million people. The New York State Department of Environmental Conservation (NYS DEC) maintains a monitoring site in Rochester, NY (43°08'46" N, 77°32'54" W, Elevation = 137 m, USEPA site code 36-055-1007). The site is adjacent to the intersection (~300 m) of two major highways (I-490 and I-590) with the annual average daily traffic (AADT) of 224,840 vehicles.<sup>15</sup> A major SO<sub>2</sub> emitter in this region, the Eastman Kodak complex, is located ~6 km northwest of the downtown area. In Monroe County, where the city of Rochester is located, RWC emissions are ranked eighth in PM<sub>2.5</sub> contributions compared with other source types. RWC emissions were estimated to be 215 tons in 2005.<sup>16</sup> There were 1867 housing units in Rochester using wood for space heating fuel in 2008.<sup>17</sup> Figure S1 shows the locations of the monitoring site, the major roadways, and emission sources in the Rochester, NY area.

Measurements of BC concentrations were made using a two-wavelength aethalometer (370 and 880 nm, Model AE-21, Magee Scientific, USA) with a time resolution of 5 min from 06/23/2008 to 02/28/2011 in Rochester, NY. The instrument aspirated the ambient air at a flow rate of 5 L/min from a height of ~5 m above the ground level. A 2.5  $\mu\text{m}$  sharp-cut cyclone inlet (BGI model SCC-1.828) excluded particles larger than 2.5  $\mu\text{m}$  from the instrument. The number concentrations of particles in 10–500 nm size range, PM<sub>2.5</sub>, CO, SO<sub>2</sub>, O<sub>3</sub>, and meteorological variables were recorded on an hourly basis during the same period.<sup>15</sup>

The number size distribution concentrations of 10–500 nm particles were measured using a scanning mobility particle sizer (SMPS), consisting of a differential mobility analyzer (DMA, model 3071, TSI Inc.), a <sup>85</sup>Kr aerosol neutralizer (model 3077, TSI Inc.), and a condensation particle counter (CPC, model 3010, TSI Inc.). Trace gas species, CO, SO<sub>2</sub>, and O<sub>3</sub>, were measured using Thermo Environmental instruments, models 48C, 43C, and 49C, respectively. Hourly PM<sub>2.5</sub> mass was measured using a Tapered Element Oscillating Microbalance (TEOM) model 1400a (Rupprecht and Patashnick now Thermo Environmental, Waltham, MA). Twenty-four-hour PM<sub>2.5</sub> integrated molecular marker samples were collected on quartz filters at this site every third day from Oct 2009 to Oct 2010. Individual organic compounds including levoglucosan, fifteen PAH species (phenanthrene, anthracene, 4H-cyclopenta[def]phenanthrene, fluoranthene, pyrene, chrysene+triphenylene, 1-methylnaphthalene, 2,6-dimethylnaphthalene, 2-methylantracene, 1-methylpyrene, retene, benzo[e]pyrene, benzo[a]pyrene, dibenz[a,h]+[a,c]-anthracene, and benzo[ghi]perylene), and fourteen vehicle exhaust markers (18 $\alpha$ (H)-22,29,30-trisnorhopane, 17 $\alpha$ (H)-22,29,30-trisnorhopane, 17 $\alpha$ (H)-21 $\beta$ (H)-29-norhopane, 18 $\alpha$ (H)-29-norhopane, 22S,17 $\alpha$ (H)-21 $\beta$ (H)-30-homohopane, 22R,17 $\alpha$ (H)-21 $\beta$ (H)-30-homohopane, 22S,17 $\alpha$ (H)-21 $\beta$ (H)-30-bishomohopane, 22R,17 $\alpha$ (H)-21 $\beta$ (H)-30-bishomohopane,

20R,5 $\alpha$ (H),14 $\beta$ (H),17 $\beta$ (H)-cholestane, 20S,5 $\alpha$ (H),14 $\beta$ (H),17 $\beta$ (H)-cholestane, 20R,5 $\alpha$ (H),14 $\alpha$ (H),17 $\alpha$ (H)-cholestane,  $\alpha\beta\beta$ ,20R,24S-methylcholestane,  $\alpha\beta\beta$ ,20R,24R-ethylcholestane, and  $\alpha\alpha\alpha$ ,20R,24R-ethylcholestane) were analyzed by gas chromatography–mass spectrometry (GC-MS).<sup>18</sup> Twenty-four-hour PM<sub>2.5</sub> potassium concentrations were obtained from the U.S. EPA speciation network.<sup>19</sup>

The aethalometer estimates the BC mass concentrations from the change of light transmission through a filter

$$ATN = -\ln\left(\frac{I}{I_0}\right) \quad (1)$$

where ATN is the attenuation,  $I_0$  is the light intensity of the incoming light, and  $I$  is the light intensity after passing through the filter. However, the relationship between ATN change and BC concentration is not linear.<sup>20</sup> As the filter gets darker (as ATN increases), the measured BC concentration is underestimated. In this study, the loading effect of aethalometer data was corrected using eq 2

$$BC_{\text{corrected}} = (1 + K \cdot ATN) \cdot BC_{\text{non-corrected}} \quad (2)$$

where  $K$  is the correction factor. The value for the factor  $K$  was calculated for each filter spot making the data continuous. The correction factor was calculated as follows

$$K_i = \frac{1}{ATN(t_i, \text{last})} \cdot \left[ \frac{BC_0(t_{i+1}, \text{first})}{BC_0(t_i, \text{last})} - 1 \right] \quad (3)$$

The  $K_i$  factor was then used to correct the BC data for both wavelengths for the filter spot  $i$  in eq 2. In practice, the  $K_i$  factors were calculated from eq 3 using the average  $BC_0$  of the last two measurements from filter spot  $i$  and the first two measurements of filter spot  $i+1$  with 5-min time resolution. This algorithm has been discussed and used in recent studies.<sup>21–23</sup>

The conditional probability function (CPF) was computed using the  $\Delta C$  values coupled with wind speed and wind direction values to identify possible locations of local sources.<sup>24</sup> In the analysis, the CPF is defined as

$$CPF_{\Delta\theta} = \frac{m_{\Delta\theta}}{n_{\Delta\theta}} \quad (4)$$

where  $m_{\Delta\theta}$  is the number of occurrences from wind sector  $\Delta\theta$  that exceeded the threshold criterion, and  $n_{\Delta\theta}$  is the total number of data points that fell within the same wind sector. In this study,  $\Delta\theta$  was set at 30°, and the threshold was set at the upper 10th percentile of the values observed at each site.

## 3. RESULTS AND DISCUSSION

**The Loading Effect Correcting Factor -  $K$ .** The average 880 nm-wavelength  $K$  factors were 0.0068, 0.0017, 0.0062, and 0.0081 for spring (Mar-May), summer (Jun-Aug), fall (Sep-Nov), and winter (Dec-Feb), respectively. The average 370 nm-wavelength  $K$  factors were 0.0054, 0.0042, 0.0054, and 0.0058 for spring, summer, fall, and winter, respectively. In summer, the  $K$  factor at 370 nm wavelength was greater compared to that for the 880 nm wavelength, which was reversed for the other three seasons (Figure S2). This wavelength-dependent seasonal variation requires further analyses of aerosol chemical composition and optical properties. These results are similar to those seen in other urban areas, which would be reasonable if the particulate

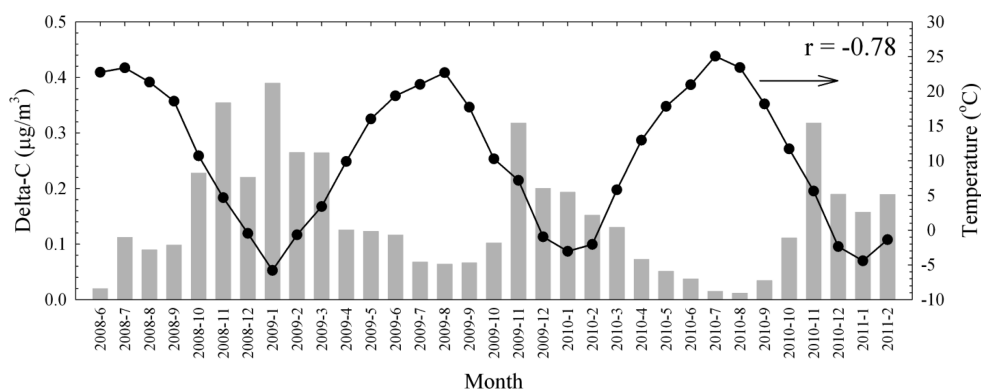


**Figure 1.** Time series plot of the monthly average Delta-C values (gray bars) and ambient temperature (solid circles). The correlation coefficient between the two variables is shown in the top-right corner.

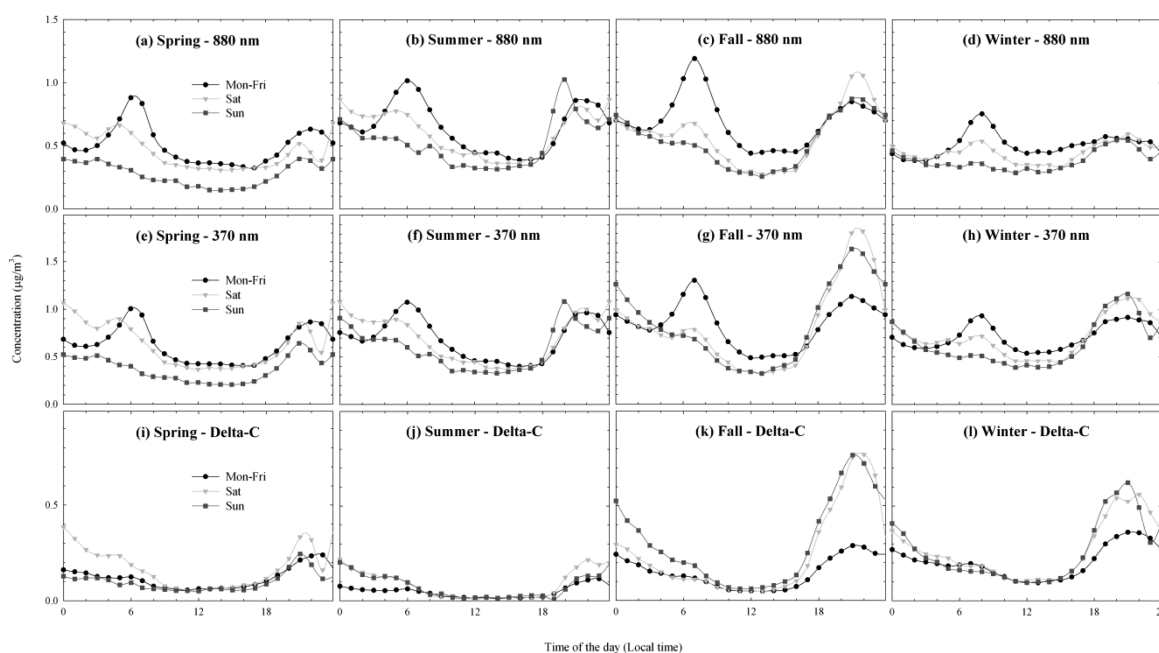


**Figure 2.** Diurnal variations of BC in 880 nm (a-d) and 370 nm (e-h) wavelengths, Delta-C (i-l) on weekdays (Monday-Friday), Saturdays, and Sundays during spring (Mar-May), summer (Jun-Aug), fall (Sep-Nov), and winter (Dec-Feb).

matter was dominated by local sources.<sup>20,22</sup> Therefore, the loading effect on the aethalometer data was corrected in further data analysis.

**The Seasonal Variations of Delta-C.** Figure 1 shows the monthly average Delta-C values and ambient temperature between Jun 2008 and Feb 2011. As expected, Delta-C is strongly linked to the season, with highest values in the colder, winter months and much lower values during the warmer, summer months. The correlation coefficient between ambient temperature and Delta-C was  $-0.78$ . The average Delta-C values were  $0.12 \mu\text{g}/\text{m}^3$ ,  $0.06 \mu\text{g}/\text{m}^3$ ,  $0.19 \mu\text{g}/\text{m}^3$ , and  $0.24 \mu\text{g}/\text{m}^3$  for spring, summer, fall, and winter, respectively (Figure S3). The summertime Delta-C was mostly attributed to remote forest fires events<sup>12</sup> and holiday firework/biomass burning activities.<sup>25</sup> A different seasonal trend for BC measured at both wavelengths is shown in Figure S3. The highest concentrations were observed during fall, while the lowest ones were during spring. The different

seasonal profile between BC and Delta-C suggests different sources contributing to these two species.

**The Diurnal Variations of Delta-C.** Figure 2 presents the diurnal pattern of BC and Delta-C on weekdays (Monday-Friday), Saturdays, and Sundays during the four seasons. The Delta-C values were elevated during the evening hours (peak around 21:00 h.) and also higher on weekends (Saturday-Sunday) compared to weekdays in spring, fall, and winter. These times correspond to periods when RWC is likely to occur. There is limited wood-burning during the work-day hours and it increases during the traditional at-home evening hours. In summer, slightly elevated Delta-C values during evening - early morning may suggest the impact of inversion-like meteorological conditions. The 880 and 370 nm BC both showed a morning peak (6:00–7:00 h.) on weekdays linked to the traffic emissions. A smaller peak was observed during evenings on both weekdays and weekends that may be due to inversions. Although BC is emitted during wood



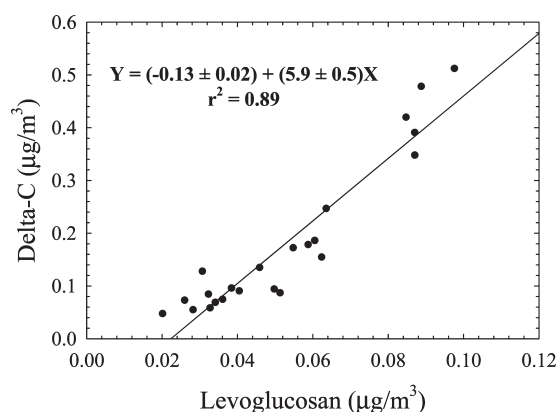


**Figure 3.** The relationship between 24-h average Delta-C and levoglucosan concentrations during winter.

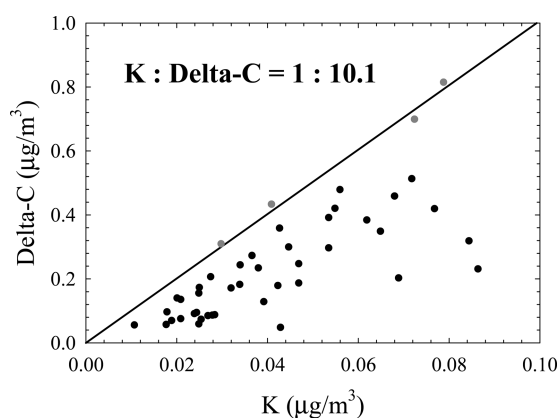


**Figure 4.** The scatter plot of 24-h average Delta-C versus elemental potassium concentrations during winter. The edge is shown by the black solid line.

combustion, it is not a robust or useful marker for RWC particles.

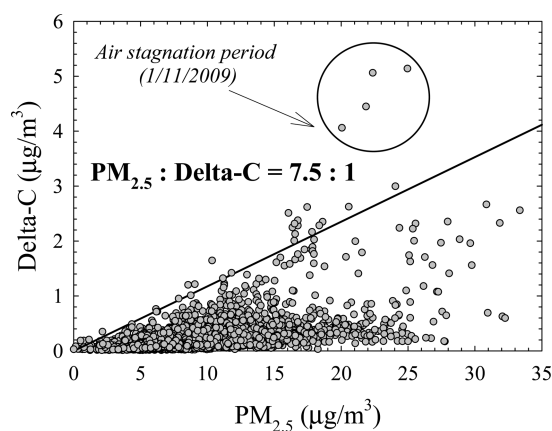
**The Correlations between Delta-C and Levoglucosan/Potassium.** To further assess the specificity of Delta-C to identify and quantify RWC PM, Delta-C is compared to the measured concentrations of levoglucosan and potassium that have been used as wood smoke markers<sup>3,26,27</sup> Seasonal variations of 24-h average levoglucosan, elemental potassium, and potassium ion concentrations are shown in Figure S4. Similar to Delta-C, the highest and lowest concentrations of levoglucosan and elemental potassium were found in winter and summer, respectively. There was no distinct seasonal trend in the potassium ion concentrations. A statistically significant linear relationship between Delta-C and levoglucosan was observed during winter ( $r^2 = 0.89$ ,  $p < 0.01$ ) as shown in Figure 3. The coefficients of determination ( $r^2$ ) between Delta-C and levoglucosan during spring, summer, and fall shown in Figure S5 were all greater than 0.57 indicating a strong correlation between these two species.

Figure S6 shows the relationship between Delta-C and elemental potassium during the four seasons. The winter  $r^2$  was 0.63, while the spring and fall  $r^2$  were 0.43 and 0.47, respectively. The summertime Delta-C and potassium showed no correlation ( $r^2 = 0.03$ ). The weaker correlation between Delta-C and potassium compared to Delta-C and levoglucosan was probably

**Table 1.** Summary of the Pearson Correlation Coefficients between Delta-C and Other Pollutants

pollutant	spring	summer	fall	winter
10–50 nm <sup>a</sup>	0.08	−0.03	0.21	0.23
50–100 nm <sup>a</sup>	0.40	0.33	0.59	0.68
100–500 nm <sup>a</sup>	0.40	0.29	0.59	0.79
BC	0.52	0.30	0.54	0.61
PM <sub>2.5</sub>	0.44	−0.01	0.41	0.51
CO	0.32	0.17	0.55	0.28
SO <sub>2</sub>	0.10	−0.03	0.01	0.04
O <sub>3</sub>	−0.37	−0.36	−0.38	−0.50

<sup>a</sup> Number concentrations of particles in 10–50 nm, 50–100 nm, and 100–500 nm size range.



**Figure 5.** The scatter plot of hourly Delta-C versus PM<sub>2.5</sub> concentrations during winter. The edge is shown by the black solid line. The circled points correspond to a temperature inversion on 1/11/2009.

due to the additional sources of potassium (e.g., crustal materials, meat cooking). The Delta-C to potassium ratio during the winter was 10.1 (Figure 4) useful for further source apportionment analysis.<sup>28</sup>

The correlation between Delta-C and phenanthrene (a PAH mainly from traffic emissions) was not statistically significant at the 99% confidence level ( $p = 0.23$ ). The correlation between Delta-C and each of the fourteen species was also calculated. The highest  $r^2$  value (0.03) was found between Delta-C and 17 $\alpha$ -(H),21 $\beta$ -(H)-29-norhopane. Since the  $p$  value in the ANOVA test is greater than 0.05, there is no statistically significant relationship between these two variables at the 95% confidence level. Delta-C and the other thirteen vehicle exhaust markers showed no correlation ( $r^2 < 0.01$ ,  $p > 0.05$ ). Therefore, Delta-C is independent of traffic emissions.

**The Correlations between Delta-C and Other Pollutants.** The Pearson correlation coefficients between Delta-C and other measured pollutants are summarized in Table 1. Winter Delta-C correlated well with the 50–100 nm ( $r = 0.68$ ) and 100–500 nm particles ( $r = 0.79$ ). It also closely related to BC concentrations during winter. Moderate negative correlations were consistently observed between Delta-C and O<sub>3</sub>. There was little correlation between Delta-C and SO<sub>2</sub> during all four seasons. Wang et al.<sup>15</sup> reported that the Eastman Kodak was one of the major SO<sub>2</sub> sources in Rochester after May 2008.

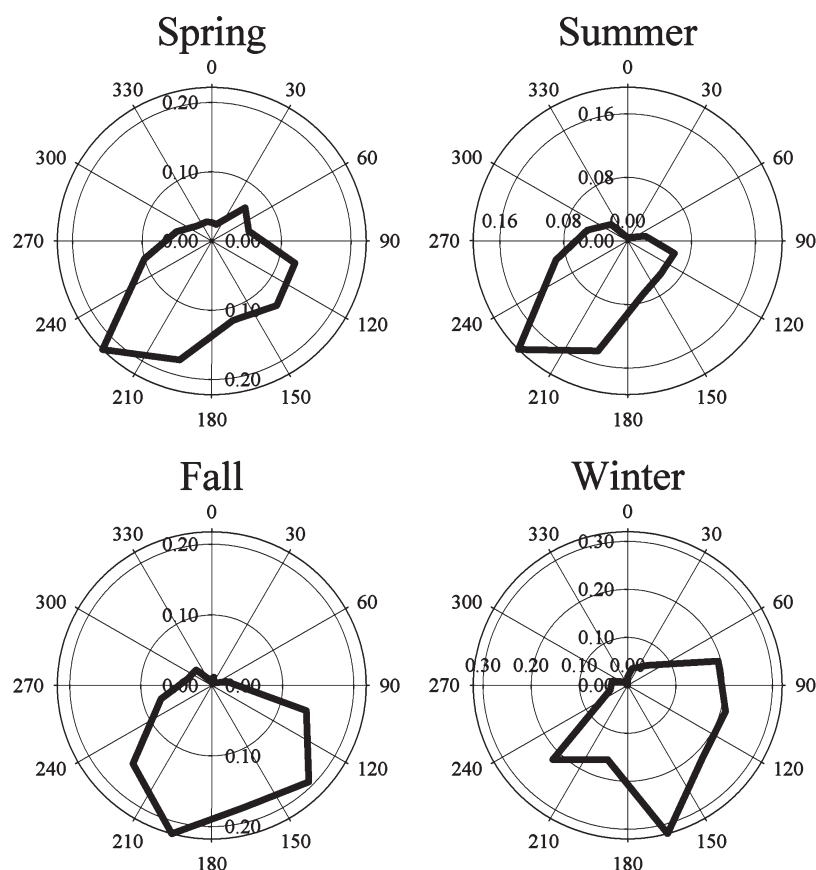


**Figure 6.** Seasonal CPF plots for the upper 10th percentile hourly Delta-C values.

A stronger correlation between Delta-C and  $\text{PM}_{2.5}$  was observed during winter ( $r = 0.51$ ) compared to summer ( $r = -0.01$ ). For those periods in winter when the hourly average  $\text{PM}_{2.5}$  concentration was greater than  $15 \mu\text{g}/\text{m}^3$ , the average Delta-C value was  $0.48 \mu\text{g}/\text{m}^3$  (average  $\text{PM}_{2.5} = 19.0 \mu\text{g}/\text{m}^3$ ), which was twice the winter average Delta-C value. In summer, the average Delta-C was  $0.05 \mu\text{g}/\text{m}^3$  when the hourly average  $\text{PM}_{2.5}$  exceeded  $15 \mu\text{g}/\text{m}^3$  (average  $\text{PM}_{2.5} = 21.9 \mu\text{g}/\text{m}^3$ ), which was close to the summertime overall average value ( $0.06 \mu\text{g}/\text{m}^3$ ). Therefore, during winter RWC particles were strongly related to the elevated  $\text{PM}_{2.5}$  concentrations. The high Delta-C values during summer were mostly from several discrete events.

Figure 5 shows the scatter plot of Delta-C vs  $\text{PM}_{2.5}$  during winter. Four data points with Delta-C values greater than  $4.0 \mu\text{g}/\text{m}^3$  were observed on 1/11/2009. Back-trajectory results indicate that the air parcel traveled from central Canada (Figure S7), where no forest fire activity was detected (Figure S8). The wind direction shifted from the north to the south with wind speed less than 1.0 m/s. The temperature dropped steadily ( $\sim -7^\circ\text{C}$ ) during the afternoon hours on 1/11/2009 (Figure S9). The RWC smoke would build up and remain at a high level under such likely inversion conditions. Pollutant concentrations started to increase around 16:00 h. and peaked around 21:00 h. CO concentration doubled from 0.4 ppm to 0.8 ppm and  $\text{PM}_{2.5}$  mass increased from  $8 \mu\text{g}/\text{m}^3$  to  $25 \mu\text{g}/\text{m}^3$ . As wind direction changed to the southwest and wind speed increased, the inversion lifted and Delta-C decreased substantially to less than  $1 \mu\text{g}/\text{m}^3$  around midnight. Thus, these extreme high winter evening Delta-C values were attributed to the combination of RWC activities

and an atmospheric inversion. All of the data shown in Figure S9 are summarized in Table S1.

An edge<sup>28</sup> with  $\text{PM}_{2.5}$  to Delta-C ratio of 7.5 was observed in Figure 5. A comparable value of 7.8 was found in multiple locations in Connecticut.<sup>29</sup> The Rochester RWC contribution to  $\text{PM}_{2.5}$  can, therefore, be estimated to be 17.3%. It increased to 27.2% when the corresponding hourly  $\text{PM}_{2.5}$  concentrations were greater than  $15 \mu\text{g}/\text{m}^3$ . Thus, RWC plays a major role in the winter ambient air pollution at this urban location.

**The Locations of Local Delta-C Sources.** CPF plots for Delta-C in spring, summer, fall, and winter are presented in Figure 6. Delta-C values are the highest from the southwest during spring and summer ( $210^\circ$ – $240^\circ$ ). In fall and winter, high Delta-C values were frequently observed from the south ( $150^\circ$ – $210^\circ$ ). The highest probability of 0.32 was found when the wind direction was  $165^\circ$  during winter. The plots point toward the residential area south of the monitoring site.

**The Effects of Snow Fall and Wind Speed on Delta-C.** Snow and ice are known to be efficient scavengers of particles.<sup>30,31</sup> Figure S10 shows the relationship between Delta-C and winter snow fall. The data collected during 18:00–5:00 h. in Dec–Feb when the wind speed was smaller than 1 m/s were included to minimize the temporal variation and the wind impact. A strong exponential decay between Delta-C and snow fall was found ( $r^2 = 0.99$ ). The Delta-C values decreased  $\sim 50\%$  when the snow fall rose from 0.0 to 0.1 cm/h.

Wind speed also affects the BC concentrations.<sup>13</sup> Figure S11 illustrates the relationship between Delta-C and wind speed.

The data collected during winter when the precipitation rate was 0.0 cm/h and the wind direction was between 60° and 240° were included. There is a clear exponential decay between Delta-C and wind speed ( $r^2 = 0.99$ ). The increase in wind speed that causes an increase in ventilation to disperse the pollutants away from the site and consequently causes a decrease in the observed Delta-C values.

**Forest Fire Transport Event.** In late May 2010, multiple forest fires ignited in southern Quebec, Canada. Transport of smoke to northern New York occurred on May 31 with impacts on local air quality. The Delta-C values were observed to significantly increase during the event. The Delta-C measurement was sensitive to forest fire smoke that has undergone significant transport.<sup>12</sup>

In this study, another high Delta-C event ( $>4.0 \mu\text{g}/\text{m}^3$ ) was observed during late afternoon – midnight on 11/23/2008 (Figure S12). The HYSPLIT backward trajectories (Figure S13) show that the origin of air parcels was central Canada, where a wide area of forest fires was detected (Figure S14). Local winds were from southwest and averaged 1 m/s during the period. Prior to 16:00 h. on November 23,  $\text{PM}_{2.5}$  mass was below  $10 \mu\text{g}/\text{m}^3$ , CO was 0.6 ppm, and BC was around  $0.5 \mu\text{g}/\text{m}^3$ . Thereafter, concentrations increased rapidly over the next few hours with  $\text{PM}_{2.5}$  mass and CO reaching  $28 \mu\text{g}/\text{m}^3$  and 1.3 ppm, respectively, around 21:00 h. The large Delta-C enhancement (from  $0.2 \mu\text{g}/\text{m}^3$  to  $5.3 \mu\text{g}/\text{m}^3$ ) is indicative of substantial wood smoke combustion PM concentration. BC at 880 nm showed another peak around 9:00 h. on November 24, but Delta-C was only  $0.7 \mu\text{g}/\text{m}^3$ . This BC peak was attributed to enhanced emissions from nearby roadways during the Monday morning commute. All of the data shown in Figure S12 are summarized in Table S2.

This work illustrates the feasibility of using Delta-C to characterize residential wood combustion particles. Delta-C was found to strongly correlate with classic wood smoke markers (levoglucosan and potassium) during the heating season. No statistically significant correlation was found between Delta-C and vehicle exhaust markers. Delta-C was particularly enhanced during the late evening on winter week-ends. Elevated concentrations during other periods were linked to emissions from remote forest fires. Compared to conventional integrated  $\text{PM}_{2.5}$  sampling and analysis, this method is simpler, cheaper, more readily accessible, and of higher time resolution for indicating the contribution level of wood smoke to atmospheric pollution. The Delta-C/ $\text{PM}_{2.5}$  ratio of 7.5 was useful for further RWC source apportionment work. RWC particles contributed 17.3% to ambient  $\text{PM}_{2.5}$  concentrations in Rochester, NY during winter.

## ■ ASSOCIATED CONTENT

**S Supporting Information.** Tables S1 and S2 and Figures S1–S14. This material is available free of charge via the Internet at <http://pubs.acs.org>.

## ■ AUTHOR INFORMATION

### Corresponding Author

\*Phone: 315-268-3861. Fax: 315-268-4410. E-mail: [hopkepk@clarkson.edu](mailto:hopkepk@clarkson.edu)

## ■ ACKNOWLEDGMENT

This work was supported by the New York State Energy Research and Development Authority (NYSERDA) through Contracts 8650 and 10604, the United States Environmental Protection Agency (EPA) through Science to Achieve Results (STAR) Grant RD83241501, a Syracuse Center of Excellence CARTI project award, which is supported by a grant from the U.S. Environmental Protection Agency [Award No: X-83232501-0], and the Electric Power Research Institute under Agreement W06325. Although the research described in this article has been funded in part by the EPA, it has not been subjected to the Agency's required peer and policy review and, therefore, does not necessarily reflect the views of the Agency and no official endorsement should be inferred. The authors also would like to thank Mr. David C. Chalupa from University of Rochester Medical Center for collecting UFP data and molecular marker samples and Tom Everts from NYSDEC for maintenance of the air monitoring instrumentation. The authors gratefully acknowledge the NOAA Air Resources Laboratory (ARL) for the provision of the HYSPLIT transport and dispersion model and the READY Web site (<http://www.arl.noaa.gov/ready.html>) used in this work.

## ■ REFERENCES

- (1) *Health effects of breathing woodsmoke*; United States Environmental Protection Agency, 2007. [http://www.epa.gov/burnwise/pdfs/woodsmoke\\_health\\_effects\\_jan07.pdf](http://www.epa.gov/burnwise/pdfs/woodsmoke_health_effects_jan07.pdf).
- (2) Ammann, H. M. Health implications of wood smoke. *Proceedings of the International Conference on Residential Wood Combustion*. Reno, NV, 1986.
- (3) Rau, J. A. Composition and size distribution of residential wood smoke particles. *Aerosol Sci. Technol.* **1989**, *10*, 181–192.
- (4) Zelikoff, J. T.; Chen, L. C.; Cohen, M. D.; Schlesinger, R. B. The toxicology of inhaled woodsmoke. *J. Toxicol. Environ. Health, Part B* **2002**, *5*, 269–282.
- (5) Pierson, W. E.; Koenig, J. Q.; Bardana, E. J. Potential adverse health effects of wood smoke. *Western J. Med.* **1989**, *151*, 339–342.
- (6) Sexton, K.; Liu, K. S.; Treitman, R. D.; Spengler, J. D.; Turner, W. J. Characterization of indoor air quality in woodburning residences. *Environ. Int.* **1986**, *12*, 265–278.
- (7) U.S. Environmental Protection Agency, 2002 national emissions inventory data and documentation. [www.epa.gov/ttnchie1/net/2002inventory.html](http://www.epa.gov/ttnchie1/net/2002inventory.html).
- (8) *Assessment of carbonaceous PM<sub>2.5</sub> for New York and the region*; report 08-01; New York State Energy Research and Development Authority (NYSERDA): Albany, NY, 2008. [http://www.nyserdera.org/programs/environment/emep/Carbonaceous\\_PM\\_2.5\\_Vol\\_II.pdf](http://www.nyserdera.org/programs/environment/emep/Carbonaceous_PM_2.5_Vol_II.pdf).
- (9) Fine, P. M.; Cass, G. R.; Simoneit, B. R. T. Organic compounds in biomass smoke from residential wood combustion: emissions characterization at a continental scale. *J. Geophys. Res.* **2002**, *107*, 8349; DOI 10.1029/2001JD000661.
- (10) Brauer, M.; Miller, P.; Allen, G. A.; Rector, L. Modeling pollution from residential wood combustion. *EM - Air Waste Manage. Assoc.* **2010**, May, 24–28.
- (11) Allen, G. A.; Babich, P.; Poirot, R. L. Evaluation of a new approach for real-time assessment of woodsmoke PM. In *Proceedings of the Regional and Global Perspectives on Haze: Causes, Consequences, and Controversies, Air and Waste Management Association Visibility Specialty Conference*, Asheville, NC, 2004, paper #16.
- (12) Wang, Y.; Huang, J.; Zhan, T. J.; Hopke, P. K.; Holsen, T. M. Impacts of the Canadian forest fires on atmospheric mercury and carbonaceous particles in northern New York. *Environ. Sci. Technol.* **2010**, *44* (22), 8435–8440.

- (13) Wang, Y.; Hopke, P. K.; Rattigan, O. V.; Zhu, Y. Characterization of ambient black carbon and wood burning particles in two urban areas. *J. Environ. Monit.* **2011**, *13*, 1919–1926.
- (14) Wang, Y.; Hopke, P. K.; Utell, M. J. Urban-scale spatial-temporal variability of black carbon and winter residential wood combustion particles. *Aerosol Air Qual. Res.*, in press.
- (15) Wang, Y.; Hopke, P. K.; Chalupa, D. C.; Utell, M. J. Long-term study of urban ultrafine particles and other pollutants. *Atmos. Environ.* **2010**; DOI 10.1016/j.atmosenv.2010.08.022.
- (16) State and county emission summaries. [http://www.epa.gov/cgi-bin/broker?\\_service=data&\\_debug=0&\\_program=dataprog.dw\\_do\\_all\\_emis\\_2005.sas&pol=231&stfips=36](http://www.epa.gov/cgi-bin/broker?_service=data&_debug=0&_program=dataprog.dw_do_all_emis_2005.sas&pol=231&stfips=36).
- (17) *Energy analysis - information, presentations and other reports/documents*; New York State Energy Research and Development Authority (NYSERDA), 2010. [http://www.nyserda.org/publications/patterns\\_trends\\_1994-2008.pdf](http://www.nyserda.org/publications/patterns_trends_1994-2008.pdf).
- (18) Simoneit, B. R. T.; Schauer, J. J.; Nolte, C. G.; Oros, D. R.; Elias, V. O.; Fraser, M. P.; Rogge, W. F.; Cass, G. R. Levoglucosan, a tracer for cellulose in biomass burning and atmospheric particles. *Atmos. Environ.* **1999**, *33*, 173–182.
- (19) Air Quality System (AQS). <http://www.epa.gov/ttn/airs/airsaqs/detaildata/downloadaqdata.htm>.
- (20) Weingartner, E.; Saathoff, H.; Schnaiter, M.; Streit, N.; Bitnar, B.; Baltensperger, U. Absorption of light by soot particles: determination of the absorption coefficient by means of aethalometers. *J. Aerosol Sci.* **2003**, *34*, 1445–1463.
- (21) Park, S. S.; Hansen, A. D. A.; Cho, S. Y. Measurement of real time black carbon for investigation spot loading effects of aethalometer data. *Atmos. Environ.* **2010**, *44*, 1449–1455.
- (22) Turner, J. R.; Hansen, A. D.; Allen, G. A. Methodologies to compensate for optical saturation and scattering in aethalometer black carbon measurements. *A&WMA Symposium on Air Quality Measurement Methods and Technology*, San Francisco, CA, 2007; paper # 37.
- (23) Virkkula, A.; Mäkelä, T.; Hillamo, R.; Yli-Tuomi, T.; Hirsikko, A.; Hämeri, K.; Koponen, I. K. A simple procedure for correcting loading effects of aethalometer data. *J. Air Waste Manage. Assoc.* **2007**, *57*, 1214–1222.
- (24) Kim, E.; Hopke, P. K.; Edgerton, E. S. Source identification of Atlanta aerosol by positive matrix factorization. *J. Air Waste Manage. Assoc.* **2003**, *53*, 731–739.
- (25) Wang, Y.; Hopke, P. K.; Rattigan, O. V. An indicator of firework emissions during the Independence Day in Rochester, New York. Under peer review.
- (26) Jordan, T. B.; Seen, A. J.; Jacobsen, G. E. Levoglucosan as an atmospheric tracer for woodsmoke. *Atmos. Environ.* **2006**, *40*, 5316–5321.
- (27) Simoneit, B. R. T. Biomass burning - a review of organic tracers for smoke from incomplete combustion. *Appl. Geochem.* **2002**, *17*, 129–162.
- (28) Henry, R. C. Multivariate receptor modeling by N-dimensional edge detection. *Chemom. Intell. Lab. Syst.* **2003**, *65*, 179–189.
- (29) *Evaluation of wood smoke contribution to particle matter in Connecticut*; Connecticut Department of Environmental Protection, Bureau of Air Management, 2011.
- (30) Lei, Y. D.; Wania, F. Is rain or snow a more efficient scavenger of organic chemicals? *Atmos. Environ.* **2004**, *38*, 3557–3571.
- (31) McLachlan, M. S.; Sellström, U. Precipitation scavenging of particle-bound contaminants — a case study of PCDD/Fs. *Atmos. Environ.* **2009**, *43*, 6084–6090.

## ■ NOTE ADDED AFTER ASAP PUBLICATION

This article published August 1, 2011 with errors throughout the text. The correct version published August 4, 2011.